

# Analytical pyrolysis-based study on intra-skeletal organic matrices from Mediterranean corals

Alessio Adamiano · Stefano Goffredo · Zvy Dubinsky · Oren Levy · Simona Fermani · Daniele Fabbri · Giuseppe Falini

Received: 28 January 2014 / Revised: 8 June 2014 / Accepted: 24 June 2014  
© Springer-Verlag Berlin Heidelberg 2014

**Abstract** Off-line analytical pyrolysis combined with gas chromatography–mass spectroscopy (GC–MS), directly or after trimethylsilylation, along with infrared spectroscopy and amino acid analysis was applied for the first time to the characterization of the intra-skeletal organic matrix (OM) extracted from four Mediterranean hard corals. They were diverse in growth form and trophic strategy namely *Balanophyllia europaea* and *Leptopsammia pruvoti*—solitary corals, only the first having zooxanthelle—and *Cladocora caespitosa* and *Astroides calycularis*—colonial corals, only the first with zooxanthelle. Pyrolysis products evolved from OM could be assigned to lipid (e.g. fatty acids, fatty alcohols, monoacylglycerols), protein (e.g. 2,5-diketopiperazines, DKPs) and polysaccharide (e.g. anhydrosugars) precursors. Their quantitative distribution showed for all the species a low protein content with respect to lipids and polysaccharides. A

chemometric approach using principal component analysis (PCA) and clustering analysis was applied on OM mean amino acidic compositions. The small compositional diversity across coral species was tentatively related with coral growth form. The presence of *N*-acetyl glucosamine markers suggested a functional link with other calcified tissues containing chitin. The protein fraction was further investigated using novel DKP markers tentatively identified from analytical pyrolysis of model polar linear dipeptides. Again, no correlation was observed in relation to coral ecology. These analytical results revealed that the bulk structure and composition of OMs among studied corals are similar, as it is the textural organization of the skeleton mineralized units. Therefore, they suggest that coral's biomineralization is governed by similar macromolecules, and probably mechanisms, independently from their ecology.

**Electronic supplementary material** The online version of this article (doi:10.1007/s00216-014-7995-1) contains supplementary material, which is available to authorized users.

A. Adamiano · S. Fermani · D. Fabbri (✉) · G. Falini (✉)  
Dipartimento di Chimica “G. Ciamician”, Alma Mater Studiorum –  
Università di Bologna, via Selmi 2, 40126 Bologna, Italy  
e-mail: dani.fabbri@unibo.it  
e-mail: giuseppe.falini@unibo.it

S. Goffredo  
Dipartimento di Scienze Biologiche, Geologiche e Ambientali,  
Alma Mater Studiorum – Università di Bologna, via Selmi 3,  
40126 Bologna, Italy

Z. Dubinsky · O. Levy  
The Mina and Everard Goodman Faculty of Life Sciences, Bar–Ilan  
University, Ramat Gan 52900, Israel

D. Fabbri · G. Falini  
Centro Interdipartimentale di Ricerca per le Scienze Ambientali,  
Sede di Ravenna - Università di Bologna, via S. Alberto 163,  
48100 Ravenna, Italy

**Keywords** Analytical pyrolysis · Biomineralization · Coral · Organic matrix · 2,5-Diketopiperazines

## Introduction

Organisms control mineral deposition by defined cellular processes that involve specific macromolecules, referred to as organic matrix (OM). These are responsible for the composition, structure and textural organization of mineralized tissues, which lead to unpaired physical and chemical properties, of which the optical and the mechanical ones are the most remarkable [1].

Biochemical analyses have revealed that skeletogenesis has a strong contribution from OM molecules showing a high content of acidic amino acids and often sugars, mostly as high-molecular-weight sulphated chains [1–4].

In the last decade, new genomic approaches have identified several tens or hundreds of genes potentially responsible for

shell formation and elevated the complexity of molecules involved in biomineralization [5]. By combining proteomic analysis with genomic and transcriptomic database interrogations, 39 proteins were identified in the shell cross-lamellar layers of the gastropod *Lottia gigantea*. Among these proteins are various low-complexity domain-containing proteins, enzymes such as peroxidases, carbonic anhydrases and chitinases, acidic calcium-binding proteins and protease inhibitors [6].

Using a similar approach based on liquid chromatography–tandem mass spectrometry analysis of proteins extracted from the cell-free skeleton of the hermatypic coral, *Stylophora pistillata*, combined with a draft genome assembly from the cnidarian host cells of the same species, 36 coral skeletal organic matrix proteins were identified. The proteome of the coral skeleton contains an assemblage of adhesion and structural proteins and two highly acidic proteins that may form a unique coral skeletal organic matrix protein subfamily [7].

Corals are simple organisms with respect to mollusks, and this is reflected also in the lower complexity of the texture of their skeletons. The fundamental structure of the coral skeleton is the “sclerodermite,” which consists of a group of aragonite elongated crystals aggregated in fascicles composed of “growth lamellae” and radiating out from a region called “centre of calcification.” Thus, the coral skeleton should be considered as a series of growth layers. The control which corals exert over the formation of the skeleton allows many corals to be identified based on the pattern of their centres of calcification and radiating fibres [8]. Thus, the coral morphology is within the species-specific “vocabulary” controlled exclusively by the taxon’s DNA. However, the signal transduction pathways and mechanisms at work are poorly understood.

The skeleton of corals is a composite structure with aragonite and OM molecules [8]. Goffredo et al. [9] showed that the intra-skeletal OM from Mediterranean solitary coral *Balanophyllia europaea* can favor the precipitation of aragonite and that a transient phase of amorphous calcium carbonate stabilized by lipids is involved. The influence of coral intra-skeletal OM molecules in the precipitation of calcium carbonate was shown also for the tropical species *Acropora digitifera*, *Lophelia pertusa* and *Montipora calculata* [10]. Moreover, an important recent study has shown that four highly acidic proteins, derived from expression of genes obtained from the common stony coral, *S. pistillata*, can spontaneously catalyze the precipitation of calcium carbonate in vitro from sea water [11].

However, despite these evidences, there are still several open questions on the extent and mechanism of control of the skeletal coral OM macromolecules on calcium carbonate precipitation, most of them due to the compositional and structural complexity of the intra-skeletal OM macromolecules.

A different approach to the understanding of skeletogenesis could be based on the research of common structural motifs in the intra-skeletal macromolecules. This approach is supported by several evidences from the genomic studies, which inferred the presence of some biomineralization genes conserved during the evolution [12].

Structural differences in the OM at a molecular level could be revealed by analytical pyrolysis and ancillary techniques (e.g. thermally assisted hydrolysis and methylation) widely applied to fingerprinting the organic matter of living organisms, for instance, in the identification of bacteria [13, 14] and fungi [15]. The application of analytical pyrolysis to the molecular characterization of organic matter involved in biomineralization has been reported for mollusks [16–18] and foraminifera [19].

Pyrolysis followed by gas chromatography–mass spectrometry (GC–MS) analysis was proposed almost 40 years ago for protein sequencing [20]. This technique offers the advantage of identifying and estimating the components of complex matrices, e.g. collagen content in archaeological bones [21] and chitin inside shrimp’s cuticle [22], from the quantification of the deriving pyrolysis products. This approach was already reported in the literature for determining specific amino acidic sequences of a protein fragment obtained from the alkaline digestion of abalone shell [18]. Particular attention was paid to the identification of 2,5-diketopiperazines (DKPs), since they form upon pyrolysis of peptides and proteins from the cyclization of two adjacent amino acids retaining their side chains [23–25].

In this study, analytical pyrolysis was applied to molecular fingerprinting of the intra-skeletal OMs extracted from four coral species from Mediterranean Sea that differ in their growth forms and trophic strategies (the presence of the symbiotic algae zooxanthellae). *B. europaea* (*Beu*) and *Leptopsamnia pruvoti* (*Lpr*) are solitary corals and only the first to have zooxanthelle. *Cladocora caespitosa* (*Cca*) and *Astroides calycularis* (*Aca*) are colonial coral with only the first having zooxanthelle. Pyrolysis data were complemented to Fourier transform infrared (FTIR) and amino acid sequence analyses to provide a comprehensive picture about the chemical nature of these coral OMs. The diversity among coral OM amino acidic compositions was evaluated by the principal component analysis (PCA) approach for complex macromolecular matrices [26–28] and clustering analysis.

## Materials and methods

### Chemicals

The linear dipeptides Gly-Glu, Gly-Asp, Gly-Ser, Asp-Asp, Asp-Glu, Glu-Asp and Glu-Glu were purchased from

GenScript USA Inc. These dipeptides were chosen based on the average acidic composition of the corals intracrystalline OM, which is very rich in glycine, serine, glutammate and aspartate (see Table 1). Bovine serum albumin (BSA), collagen, sarcosine anhydride (internal standard) and 1-benzyl-3-oxo-piperazine (silylation internal standard) were purchased from Sigma-Aldrich.

#### Coral sample preparation

Coral soft tissues were eliminated by treating the samples with a 5 % (v/v) sodium hypochlorite solution. Samples were then air dried and mechanically cleaned from rock fragments and carbonate depositions produced by other organisms. Three grams for each species was coarsely pulverized in a mortar to obtain particles of less than 1 mm of diameter. The obtained powders were then treated with a NaClO water solution (2.5 % w/w) and washed three times with Milli-Q water (resistivity 18.2 MΩ cm at 25 °C; filtered through a 0.22-μm membrane). Samples were recovered by centrifugation at 30g and left to air dry overnight. The coarsely grounded powders were then finely minced and placed in a cellulose dialysis membrane (Cellusep® T1, MWCO= 3.5 kDa) together with 25 mL of Milli-Q water. Membranes were closed and placed in a beaker with 800 mL of an aqueous solution of acetic acid at 3 % w/w to decalcify the OM. The acetic acid solution was changed twice a day for 3 days. Samples were then dialysed against Milli-Q water until this reached a pH of 6. Finally, the remaining insoluble material and solution inside the membrane were freeze-dried.

**Table 1** Mean amino acidic composition of the organic matter from the decalcification of corals

	<i>Beu</i>	<i>Lpr</i>	<i>Cca</i>	<i>Aca</i>
Asx	19.1	19.2	21.2	25.1
Gly	21.5	19.2	18.9	25.2
Arg	3.1	3.5	9.0	5.7
Ile	3.3	3.8	6.9	3.8
Phe	2.7	4.1	6.3	0.8
His	3.9	6.3	6.1	4.2
Ser	9.9	9.1	6.0	5.7
Thr	2.0	2.6	4.5	5.6
Lys	2.8	2.8	4.4	4.2
Val	4.5	5.2	4.3	5.4
Tyr	1.6	1.4	3.8	1.3
Leu	4.8	6.6	3.2	4.9
Ala	11.7	6.3	2.9	5.0
Glx	8.1	8.9	1.7	2.1
Cys	1	1	0.8	1
Met	0	0	0	0

The detection of proline and tryptophan was not possible through the used analytical procedure

#### Off-line pyrolysis

Off-line pyrolysis experiments were carried out with a heated platinum filament coil of the pyroprobe model 1000 (CDS Analytical Inc.) utilizing the procedure described in [24]. About 3–5 mg of samples was pyrolysed at a set temperature of 600 °C for 100 s at the maximum heating rate (20 °C ms<sup>-1</sup>) under nitrogen flux (200 mL min<sup>-1</sup>). Pyrolysis products were trapped onto a XAD-2 resin (orbo-43) purchased from Supelco. After pyrolysis, the cartridge was eluted with 5 mL of acetonitrile. The solutions were collected, concentrated under a gentle nitrogen stream and spiked with 0.1 mL of 250 mg L<sup>-1</sup> of sarcosine anhydride (internal standard) solution in acetonitrile before being analysed in GC–MS. An aliquot (0.1 mL) was withdrawn from the solution and subjected to the derivatization procedure for the conversion into the trimethylsilyl (TMS) derivatives, by adding 0.05 mL of 250 mg L<sup>-1</sup> of 1-oxo-3-benzopiperazine (internal standard for silylation) in acetonitrile and 0.03 mL of *N,O*-bis(trimethylsilyl) trifluoroacetamide (BSTFA) plus 1 % trimethylchlorosilane (TMCS) and heating at 60 °C for 3 h in a closed vial. The entire procedure was run in duplicate for each sample.

#### GC–MS analysis

Sample solutions were injected under splitless conditions into the injector port of an Agilent 6850 gas chromatograph connected to an Agilent 5975 quadrupole mass spectrometer. Analytes were separated by a DB-5HT (Agilent Technology) fused silica capillary column (stationary phase poly (5 % diphenyl/95 % dimethyl) siloxane, 30 m, 0.25 mm i.d., 0.25 μm of film thickness) using helium as carrier gas (at constant pressure, 33 cm s<sup>-1</sup> of linear velocity at 200 °C), with the following temperature programs: from 50 to 300 °C (held 5 min) at 5 °C min<sup>-1</sup> for the underivatized solutions, and from 100 °C (held 5 min) to 310 °C at 5 °C min<sup>-1</sup>, for the silylated solutions. The injection port was maintained at 260 °C. Mass spectra were recorded in the full scan acquisition mode under electron ionization (70 eV) at 1 scan s<sup>-1</sup> in the *m/z* 35–650 range. Relative retention times (RRTs) were calculated with respect to internal standard as  $RRT = 1 - (RT_{\text{standard}} / RT_{\text{analyte}})$ . The relative percentage compositions of coral organic matters determined by the GC–MS analysis of the underivatized pyrolysates were calculated as

$$\left[ \frac{\Sigma(A_i)}{\Sigma(A_j)} \right] \times 100$$

where  $A_i$  stands for the area of the GC–MS peak associated to the compounds of one the four classes ( $i=4$ )—namely fatty acids and lipids, polysaccharides, proteins and others—and  $A_j$

stands for the area of the GC–MS peak of every identified analyte ( $j=34$ ).

### Amino acid composition

Amino acid analysis was conducted by a chromatographic technique using an amino acid analyser. Lyophilized soluble macromolecules were hydrolyzed with 6 N HCl for 24 h at 110 °C. During hydrolysis, complete or partial destruction of several amino acids occurs: tryptophan is destroyed, and serine and threonine are partially destroyed. Sulphur amino acids are altered. Amino acid composition of the hydrolysates was also determined in duplicate by high-performance liquid chromatography (HPLC) using pre-column derivatization with *ortho*-phthalaldehyde (OPA) for primary amines and fluorometric detection. Fluorescence intensity of OPA-derivatized amino acids was monitored with an excitation wavelength of 330 nm and an emission wavelength of 450 nm.

### PCA and cluster analysis

Data analyses were performed on an Intel-Core™-based personal computer. Raw data on coral amino acidic composition, whose means are reported in Table 1, were processed by PCA and clustering analysis. Matrix dataset was composed with percentage values of amino acids as variables (columns) and corals as objects (rows). Chemometric techniques were coded and executed by authors in MATLAB R2012a, (Mathworks, Natick, USA) for windows. Euclidean distance was used for the clustering analysis. MATLAB in-house functions were used for the statistical analysis.

### FTIR spectroscopy

Spectroscopic FTIR analyses were conducted by using a FTIR Nicolet 380 (Thermo Electron Corporation) working in the range of wave numbers of 4,000–400  $\text{cm}^{-1}$  at a resolution of 2  $\text{cm}^{-1}$ . A disk was obtained mixing a small amount (<1 mg) of OM with 100 mg of KBr and applying a pressure of 48.6 psi (670.2 MPa) to the mixture using a hydraulic press.

## Results and discussion

### OM structural overview

Coral intra-skeletal OM controls the shape and the structural organization of the skeleton from the nano- to the macroscale [8]. In situ pictures of the four investigated Mediterranean coral species are shown in Fig. 1. The significant difference in the organism appearances is also associated to a diverse

textural organization of the two structural entities that form the aragonitic skeleton, the fibres and the centres of calcification (Fig. 1). Indeed, all these features are species specific and encoded in the genes of the organism. Despite these structural differences, the main features of the OM, as pictured by FTIR amino acid analysis (Fig. 2 and Table 1, respectively), do not show significant differences moving from one organism to another, even considering that they have diverse growth form (solitary vs colonial) and trophic strategy (zooxanthellate vs azooxanthellate). The FTIR spectra show in all the species the same absorption bands that differ only in their relative intensities. For the sake of clarity three zones were identified: (i) the zone 1 contains absorption bands due to vibration modes of methylene and methyl groups and thus can be associated to alkyl chains; (ii) the zone 2 contains bands due to amide group and is usually associated to proteins and acetylated polysaccharides; and (iii) the zone 3 contains bands due to vibration modes usually associated to polysaccharides. The comparison among the OMs shows in *Lpr* a higher content of alkyl chains and in *Aca* of polysaccharidic functional groups.

The amino acid analysis of OMs showed fairly the same distribution of residues. All the species, as generally observed in many mineralized tissues, showed a high content of Asx, while the content of Glx was higher in the solitary species (*Lpr* and *Beu*) with respect to the colonial one (*Acl* and *Cca*). In the latter, a higher content of Arg was observed.

The plotting of the two principal components PCA1 on PCA2—explaining together the 98.1 % of the total variance—(Fig. 3a) performed on the raw data of the amino acidic composition of coral OM ( $n=2$ ) does not show any significant difference among the species, except a not-so-evident separation of the solitary (*Beu* and *Lpr*) from the colonial (*Cla* and *Cca*) corals. The dendrogram obtained from the cluster analysis (Fig. 3b) was in line with the results obtained from PCA. This difference was mainly due to the content of alanine and serine, whose abundance was higher in solitary corals with respect to the colonial ones. These findings were in agreement with the data derived from pyrolysis (Py)/GC–MS on the protein content of corals, for which *Lpr* and *Beu* were in fact found to have similar protein content.

To get more information on the role of the primary structure of the proteins and the composition of lipids and polysaccharides, an approach based on off-line analytical pyrolysis (Py/GC–MS) has been attempted.

### Py/GC–MS of coral OM

The GC–MS profiles obtained from the pyrolysis of the intra-skeletal OM of the tested corals were remarkably similar. As an example, Fig. 4 is reported to show the GC–MS traces obtained from the pyrolysis of the decalcified skeleton of *Aca*, *Beu*, *Cca* and *Lpr*. The numbered peaks correspond to the compounds listed in Table 2 with the products reported in the

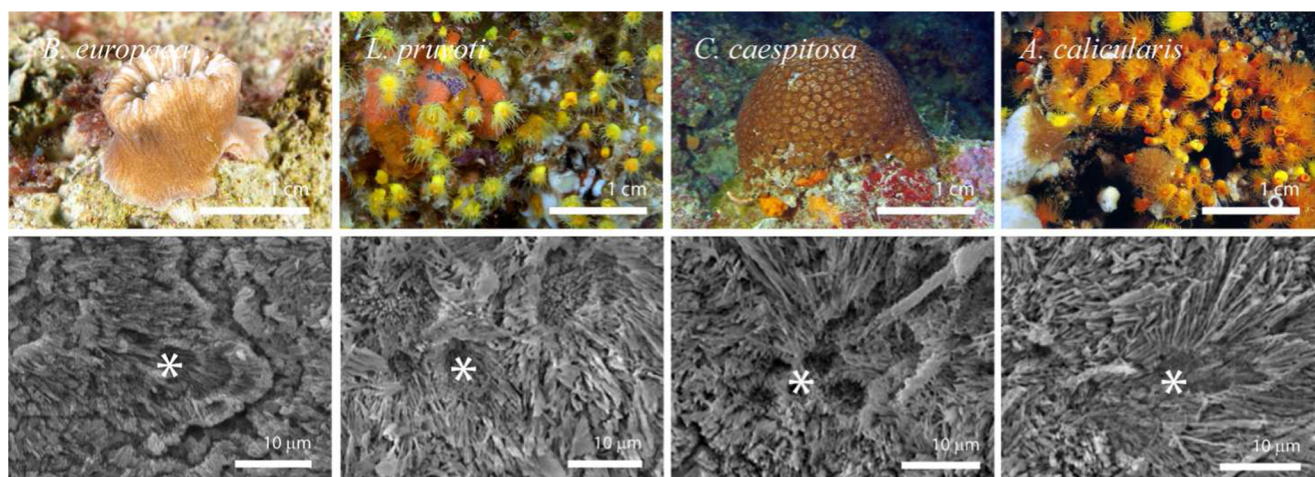


**Fig. 1** Underwater in situ camera pictures of *Beu*, *Lpr*, *Aca* and *Cca* and SEM cross-section images of their skeletons. In them, the different microscale organizations of the aragonitic fibres and of the centres of

calcification are shown. The *asterisks* indicate the centre of calcifications surrounded by fibres of aragonite

literature formed upon their pyrolysis. Besides proteins, the pyrolysis of the OM of the four corals species yielded several fatty acids (compound nos. 17 and 32–34) and other products that can be assigned to other biopolymers such as chitin and nonchitinous polysaccharides, as already reported by Stankiewicz et al. [22] for the pyrolysis of crustacean cuticle. The GC–MS-detectable compounds were classified from the matrix from which they are likely to be produced upon pyrolysis, which are the pyrolysis products of polysaccharides (PL), fatty acids and lipids (LF) and proteins (PR) (Table 2). The mean composition of coral organic matter expressed as

relative percentage of these three classes determined by means of off-line pyrolysis is summarized in Fig. 5.

#### Fatty acids and lipids

The lipid fraction (i.e. free fatty acids and lipids) was the most abundant fraction in the pyrolysate of all the studied corals. *Cca* was especially rich in this component ( $82 \pm 8\%$ ) followed by *Beu* ( $63 \pm 11\%$ ), *Aca* ( $63\% \pm 10\%$ ) and *Lpr* ( $49 \pm 12\%$ ).

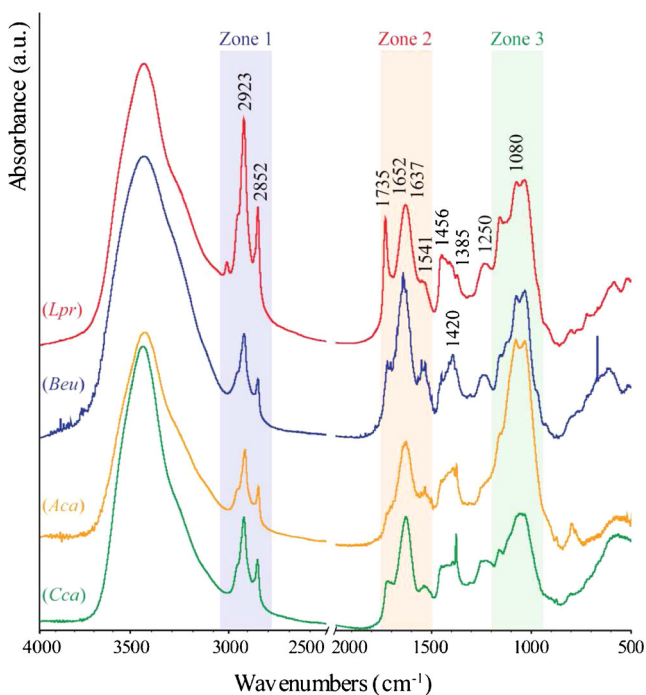


**Fig. 2** FT-IR spectra obtained from *Beu*, *Lpr*, *Aca* and *Cca*. Highlighted areas correspond to the typical adsorption bands of alkylic chains (zone 1), peptides (zone 2) and polysaccharides (zone 3)

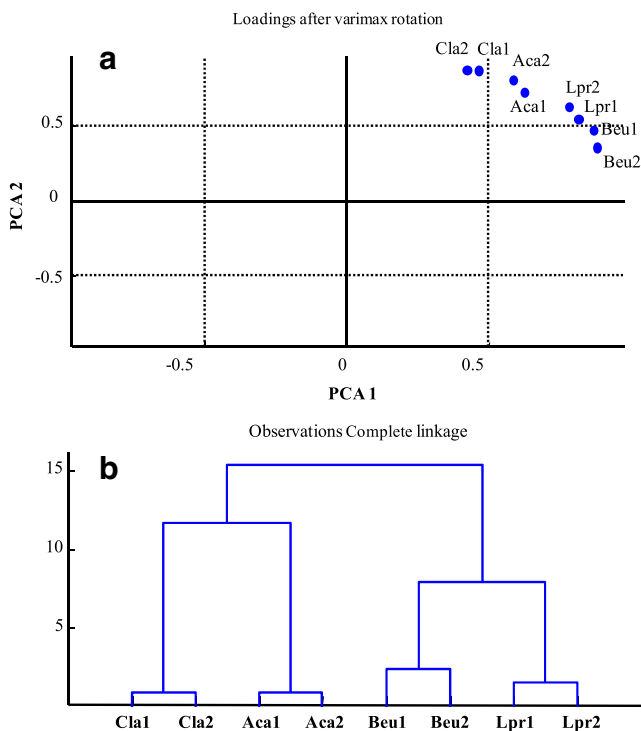


**Fig. 3** PC1/PC2 plot resulting from PCA (a) and dendrogram deriving from cluster analysis using Euclidean distance (b) performed on the amino acidic composition of *Beu*, *Lpr*, *Aca* and *Cca*

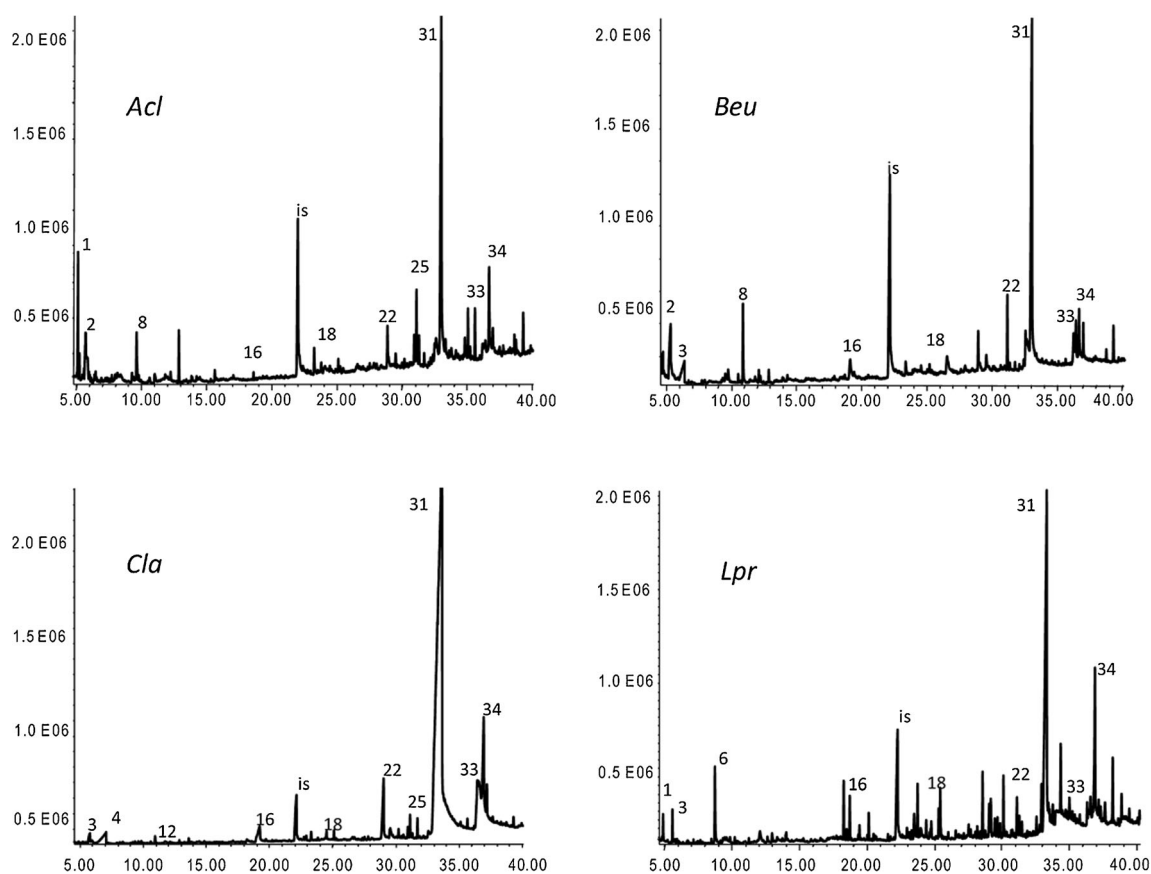


**Fig. 4** GC–MS traces obtained from analytical pyrolysis of *Beu*, *Lpr*, *Aca* and *Cca*. Peak numbers correspond to those reported in Table 2

Hexadecanoic acid was the most abundant fatty acid in all the pyrograms. This finding is according to the study by Yamashiro et al. [43] on zooxanthellate and azooxanthellate scleractinian corals and with the study by Al-Moghrabi et al. [42] on *Galaxea fascicularis*. Exceptionally high signals of 2-butenic acid were detected in *Beu* and *Cca* pyrolysates, with high signals of hexadecanoic and myristic acid. Weak peaks attributed to 2-butenic and myristic acid were detected in the GC–MS traces of *Aca* and *Lpr*. On the other hand, their pyrograms are featured by higher signals of octadecanoic acid with respect to *Beu*, but lower signals with respect to *Cca*. In summary, *Cca* was the richest species in lipids and fatty acids with respect to the other corals, with its pyrogram showing the highest signals for *n*-hexadecanoic, myristic, octadecanoic and 2-butenic acids. *Aca* and *Lpr* were rather similar, while *Beu* was found to be more similar to *Cca* in fatty acid composition. However, OM fatty acid compositions were roughly similar among these species. It is worth to notice that in contrast with that reported in the literature [42], only one unsaturated fatty acid—oleic acid (no. 33)—was detected in the tested coral specimens. This may be ascribed to the higher concentration of this compound with respect to other unsaturated fatty acids inside coral OM, which was reported for several species of scleractinian corals [43], and to the analytical technique used

in this study. However, the presence of pyrolysis products from lipids, including fatty alcohols and polyunsaturated fatty acids, could be revealed by GC–MS of the silylated pyrolysates, as described in the “Trimethylsilylation” section.

#### Polysaccharides

The peaks in the GC–MS profiles attributed to diagnostic pyrolysis products derived from polysaccharides from the coral organic matter were assigned to acetic acid (no. 1), acetamide (no. 3), 3-acetamidofuran (no. 15), *N*-(2,4-*N*-acetamido-(2,4-dihydroxyphenyl) (no. 18) and trihydro-2-acetamido-2-deoxyglucose (no. 20). Although these compounds were reported to be among the most abundant pyrolysis products produced upon chitin pyrolysis, they were detected only as minor products in all the GC–MS traces of the underivatized pyrolysates with little variations among the different species. The low abundance of chitin markers can be due to the small percentage of this biopolymer inside the coral OM, explaining also the absence of other chitin markers (e.g. 3-acetamido-4-pyrone and acetyldihydropyridine), produced in lower amounts from pure chitin pyrolysis [44]. An important point is that part of these products can be produced from the thermal degradation of non-polymerized *N*-acetylglucosamine, which is the

**Table 2** GC–MS characteristics of the principal pyrolysis products evolved from the pyrolysis of *Acl* organic matrix (OM). Classes were divided into PL=polysaccharides, L/F=fatty acids/lipidic fraction, PR=proteinaceous materials or O=others

Number	Class	Compound	RT (min)	<i>m/z</i>	Reference
1	PL	Acetic acid	5.17	56, <b>60</b>	[29, 30]
2	PL	DL-Aminoisovaleric acid	5.3	55, 57, <b>72</b> , 74 ( <i>117</i> )	[31]
3	PL	Acetamide	5.81	<b>59</b>	[32, 33]
4	L/F	2-Butenoic acid, (E)	6.33	68, 69, 71, <b>86</b>	[34]
5	L/F	2-Butenoic acid, (Z)	6.98	57, 68, 69, <b>86</b>	[34]
6	PL	2-Furancarboxaldehyde, 5-methyl	8.21	53, 81 109, <b>110</b>	[29]
7	O	(2H)-Pyridazinone, 6-methyl-	9.35	53, 68, 82, <b>110</b>	[35]
8	PR	Maleimide	9.66	54, 69, <b>97</b>	[22, 36]
9	O	3-Pyrazolidinone, 1,4-dimethyl	9.74	<b>58</b> , 69, 85, <b>114</b>	–
10	PL	1,2-Cyclopentanedione, 3-methyl-	10.5	55, 69, 103, <b>112</b>	[37]
11	PL	2-Cyclopenten-1-one, 2-hydroxy-3-methyl-	10.68	55, 69, 84, <b>112</b>	[38]
12	O	Unknown	10.93	58, 87, 113, <b>128</b>	–
13	O	Hydrouracil, 1-methyl-	12.08	57, 72, 85, <b>128</b>	–
14	PL	Levogluosenone	12.91	53, 68, 81, <b>98</b> , <b>126</b>	[38]
15	PL	3-Acetamidofuran	14.29	<b>54</b> , 82, 125	[30]
16	O	1-Hexanol, 2-mercapto-	19.08	41, <b>69</b> , 103, ( <i>134</i> )	–
17	O	Sarcosine anhydride (IS)	22.13	57, 85, 113, <b>142</b>	–
18	PL	Acetamide, <i>N</i> -(3,4-dihydroxyphenyl)-	23.31	80, 96, 125, <b>167</b>	[29]
19	L/F	Dodecanoic acid	24.57	60, <b>73</b> , 100, 129, 157, <b>200</b>	[39]
20	PL	Trihydro-2-acetamido-2-deoxyglucose	26.52	82, <b>110</b> , 125, <b>167</b>	[29]
21	PR	Pyrocoll	27.88	65, 93, 130, <b>186</b>	[20]
22	L/F	Myristic acid	28.94	60, 73, 129, 185, <b>228</b>	[40, 41]
23	PR	Cyclo(Pro-Val)	30.02	70, 72, 125, <b>154</b> , (196)	[17, 20, 22]
24	PR	Cyclo(Pro-Val)	30.66	70, 72, 125, <b>154</b> , (196)	[17, 20, 22]
25	L/F	Pentadecanoic acid	30.982	73, 129, 143, 199, <b>242</b>	[38, 40]
26	PR	Cyclo(Pro-Leu)	32.07	70, 125, <b>154</b>	[22]
27	PR	Cyclo(Pro-Leu)	32.41	70, 125, <b>154</b>	[22]
28	PR	Cyclo(Pro-Pro)	32.56	70, 96, 138, 166, <b>194</b>	[17, 20, 22]
29	PR	Cyclo(Pro-Ile)	32.63	70, 86, 125, <b>154</b> , (210)	[17, 20, 22]
30	PR	Cyclo(Pro-Ile)	32.74	70, 86, 125, <b>154</b> , (210)	[17, 20, 22]
31	L/F	<i>n</i> -Hexadecanoic acid	33.03	73, 129, 213, <b>256</b>	[39, 41]
32	L/F	Heptadecanoic acid	34.87	60, <b>73</b> , 129, 185, 227, <b>270</b>	[39, 41]
33	L/F	Oleic acid	35.64	<b>55</b> , 85, 97, 222, 264, <b>282</b>	[39, 41]
34	L/F	Octadecanoic acid	36.73	<b>73</b> , 129, 185, 241, 255, <b>284</b>	[39, 41]

monomeric unit of chitin. In addition, the presence of levogluosenone (no. 14) in all the pyrograms is interesting, which is reported in the literature to be the principal pyrolysis product of several saccharides [45]. The abundance of this compound might be derived from the decalcification process probably leading to an acid-catalyzed pyrolysis [29]; however, its presence in the GC–MS traces of all the samples shows the occurrence inside the intracrystalline OM of corals of nonchitinous polysaccharides. Since the obtained data have not enabled us to discriminate between chitin and its monomer, and between chitinous and nonchitinous polysaccharides, we decided to discuss the results as polysaccharides.

*Aca* and *Lpr* were found to have similar contents of this class of polymers, respectively  $32 \pm 10$  and  $44 \pm 5$  %. The percentage of polysaccharides in the organic matter of *Cca* was the lowest among the tested corals, its pyrolysis products accounting for only the  $9 \pm 1$  % among the compounds detected in *Cca* pyrolysate. *Beu* again was with  $17 \pm 5$  % of polysaccharide pyrolysis products. Beyond the different relative percentages detected, the same pyrolysis products were identified in each pyrogram; this supports the hypothesis of a common polysaccharidic phase inside the organic matrix of different coral species. For all the tested corals, acetamide was the most abundant product of this class, followed by acetic acid. These

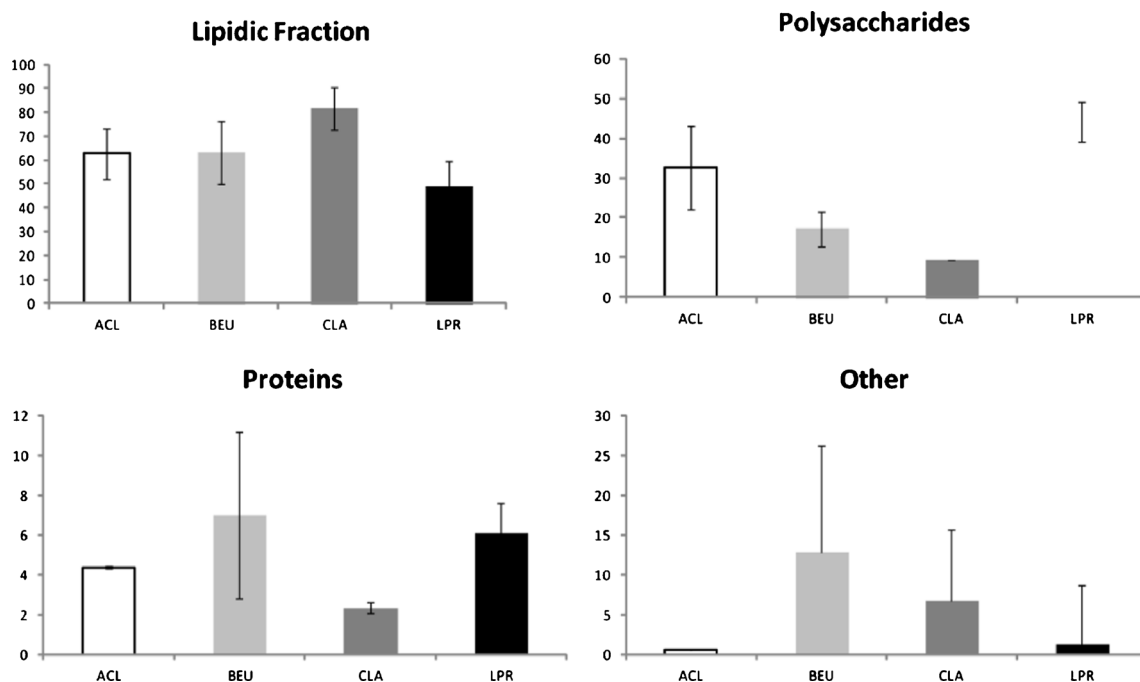


**Fig. 5** Relative percentage compositions of coral organic matters determined by Py/GC–MS calculated for each compound of the class ( $i$ ) and for every identified analyte ( $j$ ), as  $(\sum_i A_i / \sum_j A_j) \times 100$

two compounds are both reported in the literature to be formed upon chitin pyrolysis; however, acetic acid is a common pyrolysis product obtained by several biopolymers such as

wood [30] and humic matter [32], while acetamide is a typical product from pyrolysis of microbial cell walls [33] and could be formed upon pyrolysis of other precursors such as

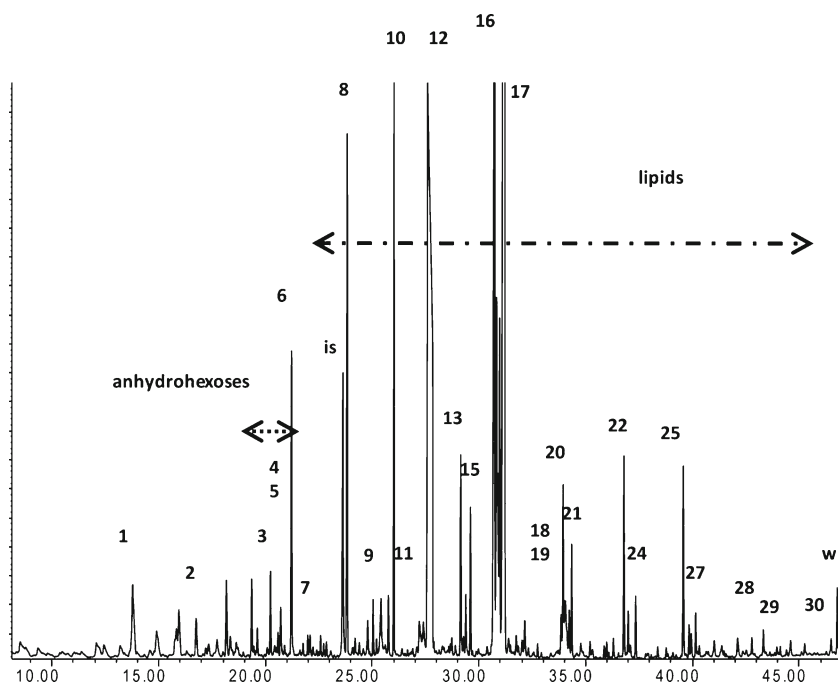


**Fig. 6** GC–MS trace of the trimethylsilylated pyrolysate of ACL organic matter. The pertrimethylsilyl derivatives of the following compounds were tentatively identified: fucosan (1); pyroglutamic acid ( $m/z$  73, 156,258); galactosan (3); mannosan (4); 1,6-anhydrogalactofuranose (5); levoglucosan (6); 1,6-anhydroglucofuranose (7); tetradecanoic (myristic) acid (8); C15 acids (9); hexadecanol (10); hexadecenoic acids (11); hexadecanoic (palmitic) acid (12); octadecen-9-ol (13); C17 acids

(14); octadecanol (15); octadecenoic acid isomers (16); octadecanoic acid (17); monomyristin (18); eicosadienoic acids (19); eicosenoic acids (20); eicosanoic acid (21); monopalmitin (22); docosenoic acid (23); docosanoic (24); monostearin (25); tetracosenoic acids (26); tetracosanoic acid (27); hexacosanoic acid (28); cholestanol (29); octadocanoic (30). hexadecanoic acid, hexadecyl ester (31)

thermally labile proteins [36]. However, the formation of these markers was attributed to the polysaccharide matrix of coral organic matter since chitin is largely present in some marine organisms (e.g. shrimps cuticle) [22].

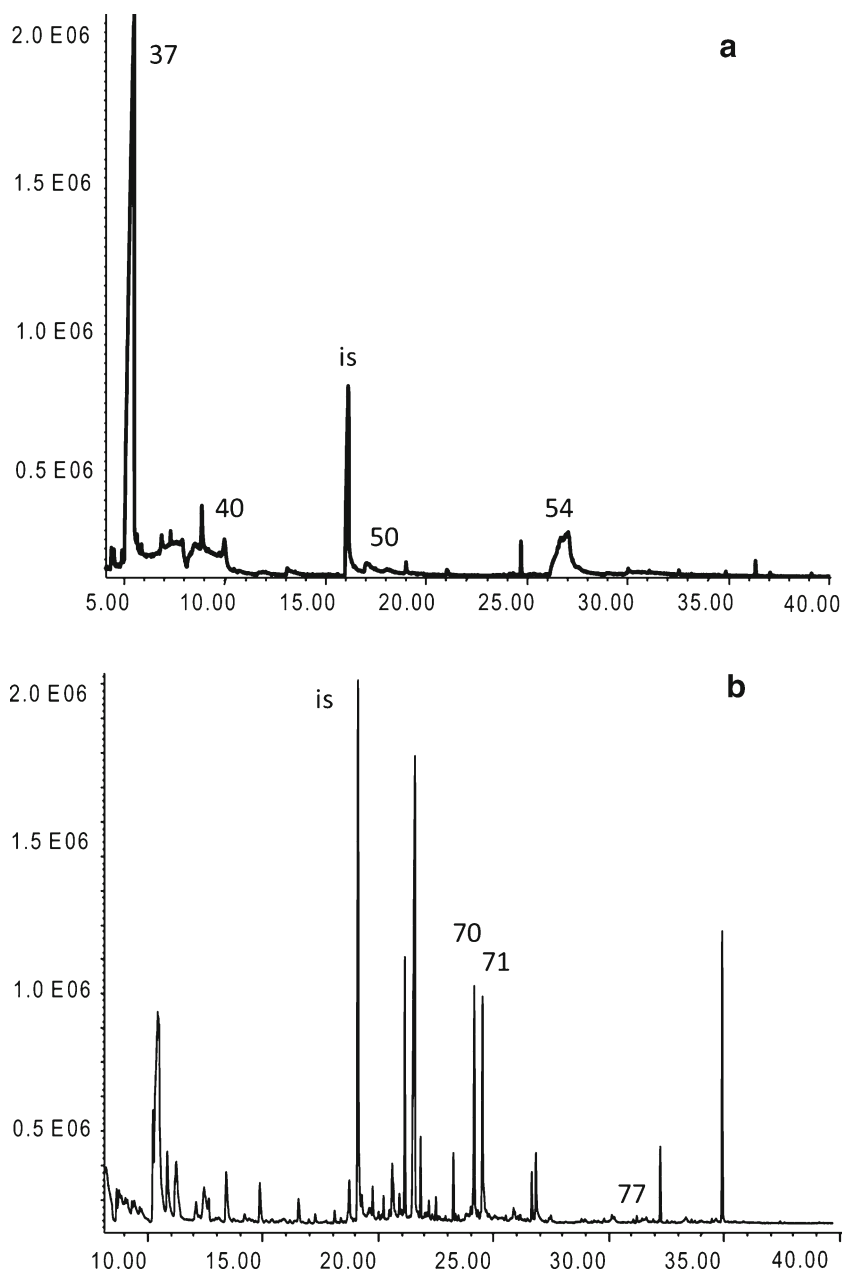
### Proteins

The highest peak assigned to the protein fraction of coral OM and detected in all the pyrolysate was that of maleimide (compound no. 18) which is the most abundant pyrolysis product of aspartate and asparagine [23]. This is according to the amino acidic composition of coral organic matter reported in Table 1, where aspartate (or asparagine, Asx), along

with glycine (Gly), was the most abundant amino acids of the OM protein fraction.

Besides, the chromatograms of all the coral samples were featured by the presence of cyclodipeptides (DKPs) containing proline (compounds nos. 23–24 and 26–30, Table 2). Proline was not reported in Table 1, because the adopted analytical method could not detect this amino acid. Interestingly, Py-GC–MS identified proline and its occurrence in sequences with valine, isoleucine and arginine. However, this finding does not imply that Pro is an abundant amino acid of OM because the thermal formation of DKPs is favored from dipeptides containing Pro [46, 47], and DKPs from Pro are rather stable [48].

**Fig. 7** GC–MS trace of the pyrolysate of the dipeptide Asp-Asp **a** as such and **b** after silylation. *Peak numbers* correspond respectively to those reported in Table 3 (**a**) and Table 4 (**b**)



No markers of polar amino acids other than maleimide were detected in the pyrolysates, even if the presence of polar amino acids inside coral OM was definitely high (Table 1). Aspartate/asparagine was the most abundant amino acid with glycine in all the samples, while glutamate (or glutamine, Glx) and serine were rather abundant in *Beu* and *Lpr* OMs. More in general, the pyrolysis products deriving from the proteinaceous matrix of coral OM accounted for the lowest fraction of the analysed pyrolysate, being its relative percentage  $4\pm 1$ ,  $7\pm 3$ ,  $2\pm 0.5$  and  $6\pm 1$  % respectively for *Aca*, *Beu*, *Cca* and *Lpr*. Considering that a great part of pyrolysis products evolving from polar amino acids eluded the GC detection, the reported relative percentage is likely to underestimate the quantities of protein inside the OM.

### Trimethylsilylation

#### Coral OM

GC–MS analysis of the silylated pyrolysates confirmed the picture emerged from the underivatized pyrograms. An example is reported in Fig. 6 with the tentative identification of the silylated products in the legend; similar chromatograms were

displayed from the other coral samples. Traces were characterized by the prominence of products from lipids, primarily fatty acid TMS esters, along with fatty alcohol TMS ethers of 14 to 18 carbon atoms. The most abundant fatty acid was hexadecanoic acid, followed by octadecanoic acid and tetradecanoic acid, and by minor amounts of fatty acids of 20, 22 and 24 carbon atoms. Unsaturated fatty acids were identified for all the fatty acid series with isomers probably formed upon thermal rearrangement of the double bonds. Fatty acids occurred probably as triacylglycerol according to the identification of TMS ethers of some monoacylglycerols. The presence of fatty alcohols and the detection of hexadecyl hexadecanoate may suggest that fatty alcohols and fatty acids may be present as waxes which are known to be major lipid components in reef-building corals [49]. Anhydrosugars indicative of monosaccharides or polysaccharides produced distinctive peaks at  $m/z$  217. They were assigned to fucosan, galactosan, mannosan and levoglucosan [50], all compounds known to be components of the soluble organic matter of zooxanthellate and azooxanthellate scleractinian corals [51]. Two small peaks at the anhydrosugar elution region (at 23.7 and 24.3 min) and mass spectra with characteristic ions at  $m/z$  131, 186 and 173 were attributed to dehydrated monomers of chitin [31].

**Table 3** GC–MS characteristics of pyrolysis products evolved from the pyrolysis of polar amino acids containing linear dipeptides

Number	Molecular attribution	RRT	$m/z$	Sample
35	Maleic anhydride	−3.39	<b>54</b> , 98	Glu-Asp
36	2,5-Furandione	−3.36	54, <b>98</b>	Asp-Glu
37	Maleimide, <i>N</i> -ethyl	−2.27	<b>69</b> , 82, 97, 110, 125	Asp-Asp
38	Oxazole, 2-phenyl	−2.22	51, 90, 117, <b>145</b>	Gly-Glu, Glu-Glu
39	Maleimide	−1.93	54, 69, <b>97</b>	Gly-Asp, Glu-Glu, Asp-Asp, Glu-Asp, Asp-Glu
40	Succinimide	−0.87	56, 69, <b>99</b>	Asp-Asp, Gly-Glu, Glu-Glu
41	Pyrimidine, 2,4,5-triamino-	−0.67	56, 69, 98, <b>125</b>	Glu-Asp
42	Methyl succinimide	−0.61	56, 70, <b>99</b> , 114	Asp-Asp
43	1,2,6-Dioxohexahydropyrimidine carboxylic acid	−0.59	70, 95, <b>113</b>	Asp-Glu
44	Hydroxyproline derivative (A)	−0.5	58, 69, <b>86</b> , 113	Asp-Glu, Glu-Asp
45	Alkyl pyrrolidine-2-one	−0.46	51, 69, 110	Gly-Asp
46	Hydroxyproline derivative (B)	−0.42	58, 69, <b>86</b> , 113, 139	Asp-Glu, Glu-Asp
47	Hydroxyproline derivative (C)	−0.26	58, 69, <b>86</b> , 113, 139	Asp-Glu, Glu-Asp
48	2-Pyrrolidinecarbonitrile	−0.14	56, 67, <b>110</b>	Glu-Glu
49	Pyrrolidine-1-acetonitrile	−0.06	<b>54</b> , 69, 138	Gly-Asp
50	Succinimide, <i>N</i> -alkyl	0.05	69, <b>139</b> , 167	Asp-Asp
51	Cyclo(Gly-Ser)	0.2	57, <b>85</b> , 114, 127	Gly-Ser
52	Pyroglutamic acid	0.28	28, 41, 56, <b>84</b> , 129	Glu-Glu
53	Alkyl,pyrrolidin-2-one	0.35	56, 69, 77, <b>84</b>	Gly-Glu
54	Maleimide dimer	0.39	55, 97, <b>125</b> , 153, 196	Asp-Asp
55	Pyrrolizin-1,7-dione-6-carboxylic acid methyl ester	0.44	55, 69, <b>84</b> , 156, (197)	Glu-Glu
56	Pyroglutamic derivative	0.46	55, 69, <b>84</b>	Glu-Glu
57	Cyclo(PyroGlu-Gly)	0.47	56, <b>84</b> , 97, 126, 168	Gly-Glu

RRT retention time relative to sarcosine anhydride

### Linear dipeptides

To gather more information on the protein fractions of corals characterized by the sequence of polar amino acids, a detailed study was conducted on the pyrolytic behavior of pure linear dipeptides formed by polar amino acids with the objective to identify diagnostic pyrolysis products. The analysed linear dipeptides were various (not all the possible) combinations of aspartate, glutamate, serine and glycine, the latter being the predominant nonpolar amino acid in the OM. As an example, the GC–MS traces of Asp-Asp pyrolysate before and after silylation are shown in subpanels a and b of Fig. 7, respectively. The GC–MS profiles of the underivatized pyrolysates were featured by few broad peaks with low intensities. Thus, a silylation procedure was mandatory to improve their GC analysis [24]. The tentative identification of the pyrolysis products is discussed in the Electronic Supplementary Material (ESM).

The principal pyrolysis products tentatively identified in the pyrograms obtained from the underivatized pyrolysates of the dipeptides are listed in Table 3. They were reported to be formed upon single amino acid pyrolysis, and so they cannot be considered as specific markers of dipeptidic sequences. Among these, the most abundant in all the pyrolysate of the studied corals were maleimide, succinimide and pyroglutamic acid. The first two compounds are well known to be formed upon aspartic acid pyrolysis, while pyroglutamic is known to be formed from the thermal degradation of glutamic acid and glutamine.

On the contrary, the analysis of the silylated pyrolysate of dipeptides revealed the presence of several compounds tentatively identified as trimethylsilyl derivatives of DKPs, thus indicative of polar amino acid sequences (Table 4). The silylated pyrogram of *Acl*, the cyclic dipeptides associated to the thermal degradation of the sequence of Gly-Ser, Gly-Asp, Gly-Glu and Glu-Glu, were identified. Unexpectedly, *Acl* was the only sample for which markers of Gly-Glu and Glu-Glu were detected, though the percentage of glutamic acid/glutamate in its OM was rather low (2.2 % Table 1) with respect to that of *Beu* and *Lpr* (8.1 and 8.9 %, respectively). DKPs associated to the Asp-Asp sequences were identified in the OMs of *Beu*, *Cca* and *Lpr*. Besides, DKPs derived from Gly-Ser were detected in the pyrograms of *Beu* and *Cca*. Thus, it was demonstrated that Py/GC–MS can provide preliminary information of the amino acid connectivity through the identification of thermally produced cyclic dipeptides; however, a detailed protein sequencing of OM needs specific analytical techniques, such as LC-MS/MS, supported by careful sample pretreatments and informatics platform, yet rarely applied to corals [7].

### Conclusions

For the first time, Py/GC–MS in combination with amino acid analyses and FT-IR was applied to characterize the complex

**Table 4** GC–MS characteristics of tentatively identified silylated DKPs deriving from the pyrolysis of pure dipeptides containing polar residues and their presence in the pyrolysate of coral OM. RRT denotes retention

Number	RRT	<i>m/z</i>	Sample	DKP	<i>Acl</i>	<i>Beu</i>	<i>Cca</i>	<i>Lpr</i>
59	−0.98	73, 129, 142, <b>257</b> , 272	Gly-Ser	Di-TMS cyclo(Gly-Ala)	+	+	−	+
60	−0.91	73, 113, 127, <b>258</b> , 287	Gly-Asp, Gly-Ser	Di-TMS cyclo(Gly-Ser)	−	−	−	−
61	−0.87	73, <b>100</b> , 243, 258	Gly-Asp	Di-TMS cyclo(Gly-Gly)	−	−	−	−
62	−0.24	73, 147, <b>257</b> , 345, 360	Gly-Ser	Tri-TMS cyclo(Gly-Ser)	−	+	−	−
63	−0.14	<b>83</b> , 111, 211, 226	Glu-Glu	Mono TMS 1-ethen-4-methyl-2,5-diketopiperazine	−	−	−	−
64	−0.02	73, 156, <b>271</b> , 373, 388	Gly-Asp	Tri-TMS cyclo(Gly-Asp)	+	−	−	+
65	0.03	73, 168, 241, 297, <b>312</b>	Gly-Glu	Mono-TMS cyclo(PyroGlu-Gly)	−	−	−	−
66	0.07	73, 157, 168, <b>240</b>	Gly-Glu	Mono-TMS cyclo(PyroGlu-Gly)	−	−	−	−
67	0.13	73, <b>156</b> , 386	Asp-Glu, Glu-Asp	Di-TMS cyclo(Asp-Glu)-H <sub>2</sub>	−	−	−	−
68	0.14	73, <b>156</b> , 386	Asp-Glu, Glu-Asp	Di-TMS cyclo(Asp-Glu)-H <sub>2</sub>	−	−	−	−
69	0.19	73, 127, <b>156</b> , 369, 384	Gly-Glu, Glu-Glu	Di-TMS cyclo(Glu-pyroGlu)	+	−	−	−
70	0.21	73, 100, 155, 171, 199, <b>325</b> , 340	Asp-Asp	Di-TMS cyclo(Asp-Asp)-2H <sub>2</sub> O	−	+	+	+
71	0.22	73, 100, 155, 171, 199, <b>325</b> , 340	Asp-Asp	Di-TMS cyclo(Asp-Asp)-2H <sub>2</sub> O	−	+	+	+
72	0.29	73, 127, <b>156</b> , 369, 384	Gly-Glu, Glu-Glu	Di-TMS cyclo(Glu-pyroGlu)	−	−	−	−
73	0.36	73, 129, 169, 217, <b>476</b>	Glu-Asp	Uncertain	−	−	−	−
74	0.36	73, 129, 169, 217, <b>476</b>	Glu-Asp	Uncertain	−	−	−	−
75	0.37	73, 129, 169, 217, <b>476</b>	Glu-Asp	Uncertain	−	−	−	−
76	0.37	73, 129, 169, 217, <b>476</b>	Glu-Asp	Uncertain	−	−	−	−
77	0.41	73, 100, 172, 287, 359, <b>374</b> ( <i>M-H</i> )	Asp-Asp	Di-TMS cyclo (Asp-Asp)	−	+	+	+

time relative to the trimethylsilylated derivative of 1-benzo-3-oxo-piperazine. In the last four columns, the DKPs respectively detected in the organic matter of each coral species are indicated by (+)

OM of four different species of Mediterranean Sea corals. The compounds produced upon pyrolysis of coral-extracted OM were classified in fatty acids and lipids, proteins and polysaccharides consistently with FTIR spectra. According to analytical pyrolysis, the major components were lipids (C14–C24 fatty acids, C14–C18 fatty alcohols, triacylglycerols and waxes) and saccharides (mannose, galactose and glucose derivatives), independently from the coral source. Interestingly, in such matrix, the presence of *N*-acetyl glucosamine in polymerized forms was observed. The DKPs detected in the pyrograms were consistent with the amino acidic composition of each coral and provided additional information on the primary sequence showing the presence of proline and that, despite the high content of Asp, sequences of this amino acid were not predominant and even absent in *Cca* OM. Moreover, the application of a chemometric analysis to the amino acid composition revealed a small diversity related to the growth form and not to the trophic strategy.

The impact of these results in the understanding of coral biomineralization is significant. The proteins, which have been considered for a long time the main controllers of the mineralization process, appear as a minor component of the OM. This observation gives a significant role to lipids and polysaccharides, which have been reported to be involved in the stabilization of transition phases (i.e. amorphous calcium carbonate) during the aragonitic skeleton formation [8]. Among sugars the presence of *N*-acetyl-glucosamine links corals to other mineralized tissues (like shells and radula), where chitin plays an important role in the biomineralization process [1]. The information obtained from the primary sequence of the protein regions, despite the difference observed, could not be correlated with the growth form and the trophic strategy of the coral. This data, together with the information on the macromolecular distribution, suggests that coral biomineralization is poorly linked with the above parameters, according to the similarities reported, and observed, of the coral mineral components, fibres and centres of calcification, in distribution and texture.

**Acknowledgments** The research leading to these results has received funding from the European Research Council under the European Union's Seventh Framework Programme (FP7/2007-2013)/ERC grant agreement no. [249930–CoralWarm: Corals and global warming: the Mediterranean versus the Red Sea]. We deeply thank Gianni Neto for the coral underwater pictures. GF and SF thank the Consorzio Interuniversitario di Ricerca della Chimica dei Metalli nei Sistemi Biologici (CIRC MSB) for the support.

## References

- Lowenstam HA, Weiner S (1989) On biomineralization. Oxford University Press, Oxford
- Addadi L, Joester D, Nudelman F, Weiner S (2006) *Chem Eur J* 12: 981–987
- Weiner S, Addadi L (2011) *Annu Rev Mater Res* 41:21–40
- Falini G, Fermani S (2013) *Cryst Res Technol* 48:864–876
- Marin F, Le Roy N, Marie B (2012) *Front Biosci* 4:1099–1125
- Marie B, Jackson DJ, Ramos-Silva P, Zanella-Cleon I, Guichard N, Marin F (2013) *FEBS J* 280:214–232
- Drake JL, Mass T, Haramaty L, Zelzion E, Bhattacharya D, Falkowski PG (2013) *Proc Natl Acad Sci U S A* 110:2147–2148
- Tambutté S, Holcomb SM, Ferrier-Pagès C, Reynaud S, Tambutté É, Zoccola D, Allemand D (2011) *J Exp Mar Biol Ecol* 408:58–78, and references therein
- Goffredo S, Vergni P, Reggi M, Caroselli E, Sparla F, Levy O, Dubinsky Z, Falini G (2011) *PLoS ONE* 6:e22338
- Falini G, Reggi M, Fermani S, Sparla F, Goffredo S, Dubinsky Z, Levi O, Dauphin Y, Cuif JP (2013) *J Struct Biol* 183:226–238
- Mass T, Drake JL, Haramaty L, Kim JD, Zelzion E, Bhattacharya D, Falkowski PG (2013) *Curr Biol* 23:1126–1131
- Mann K, Wilt FH, Poustka AJ (2010) *Proteome Sci* 8:33
- Voorhees KJ, Basile F, Beverly MB, Abbas-Hawks C, Hendricker A, Cody RB, Hadfield TL (1997) *J Anal Appl Pyrol* 40–41:111–134
- Prasad S, Schmidt H, Lampen P, Wang M, Güth R, Rao JV, Smith GB, Eiceman GA (2006) *Analyst* 131:1216–1225
- Schwarzinger C (2005) *J Anal Appl Pyrol* 74:26–32
- Furuhashi T, Schwarzinger C, Miksik I, Smrz M, Beran A (2009) *Comp Biochem Phys B* 154:351–371
- Furuhashi T, Beran A, Blazso M, Czegeny Z, Schwarzinger C (2009) *Biosci Biotechnol Biochem* 73:93–103
- Adamiano A, Bonacchi S, Calonghi N, Fabbri D, Falini G, Fermani S, Genovese D, Kralj D, Montalti M, Džakula N, Prodi L, Sartor G (2012) *Chem Eur J* 18:14367–14374
- NiFlhaithearta S, Ernst SR, Nierop KGJ, de Lange GJ, Reichart GJ (2013) *Mar Micropaleontol* 102:69–78
- Johnstone RAW, Povall TJ (1975) *JCS Perkin I*, pp:1297–1300
- Adamiano A, Fabbri D, Falini G, Belcastro MG (2013) *J Anal Appl Pyrol* 100:173–180
- Stankiewicz BA, Mastalerz M, Hof CHJ, Bierstedt A, Flannery MB, Briggs DEG, Evershed RP (1998) *Org Geochem* 28:67–76
- Chiavari G, Galletti G (1992) *J Anal Appl Pyrol* 24:123–137
- Fabbri D, Adamiano A, Falini G, Mancini I, De Marco R (2012) *J Anal Appl Pyrol* 95:145–155
- Templier J, Gallois N, Derenne S (2013) *J Anal Appl Pyrol*. doi:10.1016/j.jaap.2013.09.017
- Sciutto G, Oliveri P, Prati S, Quaranta M, Lanteri S, Mazzeo R (2013) *Anal Bioanal Chem* 405:625–633
- Xu Y, Cheung W, Winder CL (2010) *Anal Bioanal Chem* 397:2439–2449
- Lu Y, Harrington PB (2010) *Anal Bioanal Chem* 397:2959–2966
- Torri C, Lesci IG, Fabbri D (2009) *J Anal Appl Pyrol* 85:192–196
- Alén R, Kuoppala E, Oesch P (1996) *J Anal Appl Pyrol* 36:137–148
- Fabbri D, Prati S, Vassura I, Chiavari G (2003) *J Anal Appl Pyrolysis* 68–69:163–171
- Abelenda MS, Buurman P, Arbestain MC, Kaal J, Martinez-Cortizas A, Gartzia-Bengoetxea N, Macías F (2011) *Eur J Soil Sci* 62:834–848
- Cao JP, Zhao XY, Morishita K, Wei XY, Takarada T (2010) *Bioresour Technol* 101:7648–7652
- Schlottzauer WS, Choratyk OT, Austin PR (1976) *J Agric Food Chem* 24(1):177–180
- Ratcliff MA Jr, Medley EE, Simmonds PG (1974) *J Org Chem* 39: 1481–1490
- Sharma RK, Chan WG, Wang J, Waymack BE, Wooten JB, Seeman JI, Hajaligol MR (2004) *J Anal Appl Pyrol* 72:153–163
- Schulten HR (1999) *J Anal Appl Pyrol* 49:385–415
- Räisänen U, Pitkänen I, Halttunen H, Hurttta M (2003) *J Therm Anal Calorim* 72:481–488
- Fabbri D, Torri C, Baravelli V (2007) *J Anal Appl Pyrol* 80:24–29

40. Gelencsér A, Mészáros T, Blazsó M, Kiss GY, Krivácsy Z, Molnár A, Mészáros E (2000) *J Atmos Chem* 37:173–183
41. Casol A, Mirti P, Palla G (1995) *Fresenius J Anal Chem* 352:372–379
42. Al-Moghrabi S, Allemand D, Couret JM, Jaubertal J (1995) *J Comp Physiol B* 165:183–192
43. Yamashiro H, Hirotsuke O, Higa H, Chinen I, Sakai K (1999) *Comp Biochem Phys B* 122:397–407
44. Stankiewicz BA, Briggs DEG, Evershed RP, Flannery MB, Wuttke M (1997) *Science* 276:1541–1543
45. Schulten HR, Sorge-Lewin C, Schnitzer M (1997) *Biol Fertil Soils* 24:249–254
46. Richmond-Aylor A, Bell S, Callery P, Morris K (2007) *J Forensic Sci* 52:380–382
47. Smith GG, Reddy GS, Boon JJ (1988) *J Chem Soc Perkin Trans II*: 203–211
48. Fischer PM (2003) *J Pept Sci* 9:9–35
49. Imbs AB (2013) *Russ J Mar Biol* 39:153–168
50. Torri C, Soragni E, Prati S, Fabbri D (2013) *Microchem J* 110:719–725
51. Gautret P, Cruit JP, Freiwald A (1997) *FACIES* 36:189–194